

$|V_{ub}|$ and $|V_{cb}|$ from CLEO

A. Bornheim

(representing the CLEO Collaboration^a)

Caltech, Lauritsen Laboratory, 1200 E. California Blvd. , Pasadena CA, 91125, USA



We report on studies of exclusive and inclusive semileptonic $b \rightarrow u\ell\nu$ and $b \rightarrow c\ell\nu$ decays in 9.7 million $B\bar{B}$ events accumulated with the CLEO detector in symmetric e^+e^- collisions produced in the Cornell Electron Storage Ring (CESR). Various experimental techniques, including the inference of neutrino candidates using the hermeticity of the CLEO detector and the study of spectral moments, are used in conjunction with theoretical calculations to provide estimates of the CKM matrix elements $|V_{ub}|$ and $|V_{cb}|$.

1 Introduction

One of the main goals of B-physics is to test the consistency of the standard model (SM) description of quark mixing¹. In the Wolfenstein representation² the quark mixing matrix is described by four parameters. Two of the free parameters, ρ and η , are commonly pictured as the Unitarity Triangle. The ρ - η parameter space is constrained by various B-physics and K-physics measurements in different ways as shown in Fig. 1.

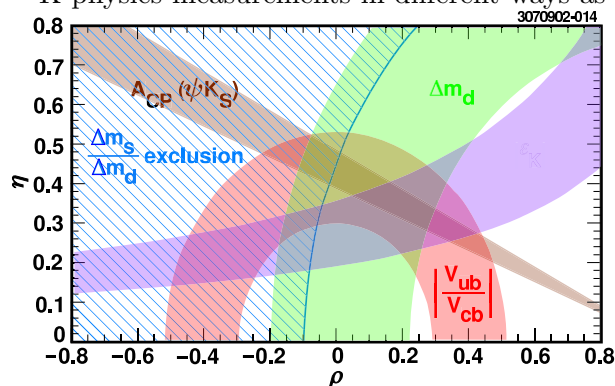


Figure 1: The ρ - η plane showing the constraints on these two parameters from various measurements in B- and K-physics. The ratio of the measurements of $|V_{ub}|$ and $|V_{cb}|$ we report on in this document provide a donut-shaped constraint around the origin. The measurement of $A_{CP}(\Psi/K_s)$ performed by the Belle and BaBar collaborations is currently still statistically limited as is the measurement of $\frac{\Delta m_s}{\Delta m_d}$ which will be improved with the upcoming results from the Tevatron run II. The measurement of $|\epsilon_K|$ is systematically limited.

^aPresented at the XXXVIII. Rencontres de Moriond, Electroweak Interactions and Unified Theories

All these measurements pose very different experimental, phenomenological and theoretical challenges. To measure $|V_{ub}|$ and $|V_{cb}|$ one has to measure decay rates corresponding to the quark-level transitions $b \rightarrow u$ and $b \rightarrow c$. In practice the problem is that the measurements of these rates are obscured by hadronization effects and interactions between initial and final state particles involved. Since no reliable method exists to date to fully calculate these effects one has to control them in other ways. One common approach is to use semileptonic decays $B \rightarrow X_u l \nu$ and $B \rightarrow X_c l \nu$ which reduce non-calculable hadronic effects considerably. Furthermore one measures $|V_{ub}|$ and $|V_{cb}|$ in many different ways in order to get a better handle on the remaining non-perturbative effects. Finally one uses calculations, in particular from heavy quark effective theory (HQET)⁴ and lattice QCD (LQCD)⁵, to link various measurements together to further reduce theoretical uncertainties. In the following we give an overview of the $|V_{ub}|$ and $|V_{cb}|$ measurements performed with the CLEO detector³ at the CESR e^+e^- collider.

2 Measurements of $|V_{cb}|$

2.1 $|V_{cb}|$ exclusive

Using exclusive $B \rightarrow D^* l \nu$ decays one can employ heavy quark symmetry relations to calculate strong interaction form factors that enter the decay rate. In the framework of HQET it is useful to consider the kinematic variable $w = v_B \cdot v_{D^*} = \frac{m_B^2 + m_{D^*}^2 - q^2}{2m_B m_{D^*}}$, which is linearly related to q^2 , the mass of the virtual W . The decay rate can then be written as $\frac{d\Gamma}{dw} = \frac{G_F^2}{48\pi^3} |V_{cb}|^2 [\mathcal{F}(w)]^2 \mathcal{K}(w)$ where $\mathcal{K}(w)$ is a kinematic function of the masses and the variable w depends only on the V-A structure of the weak transition. $\mathcal{F}(w)$ is a form factor representing the strong interaction dynamics of the $B \rightarrow D^*$ transition⁷. In HQET $\mathcal{F}(w)$ can be calculated for $w = 1$; Lattice QCD and QCD sum rules give similar results⁶. The shape of the form factor is less determined, QCD dispersion relation may be used to constrain it⁷. Experimentally one measures the decay rate as a function of w and extrapolates back to $w = 1$ where $\mathcal{F}(1)|V_{cb}|$ can then be extracted. In Fig. 2 the measured rates are shown for $D^{*+} l \nu$ (top) and $D^{*0} l \nu$ (center). The bottom plot shows the fit to the values of $|V_{cb}|^2 \mathcal{F}(w)$ derived from the corrected rates for both $D^{*+} l \nu$ and $D^{*0} l \nu$.

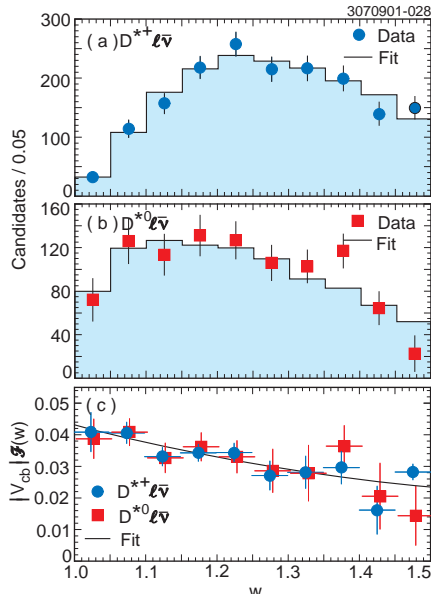


Figure 2: $D^* l \nu$ rate for charged (top) and neutral (center) D^* and $|V_{cb}| \mathcal{F}(w)$ as a function of w (bottom).

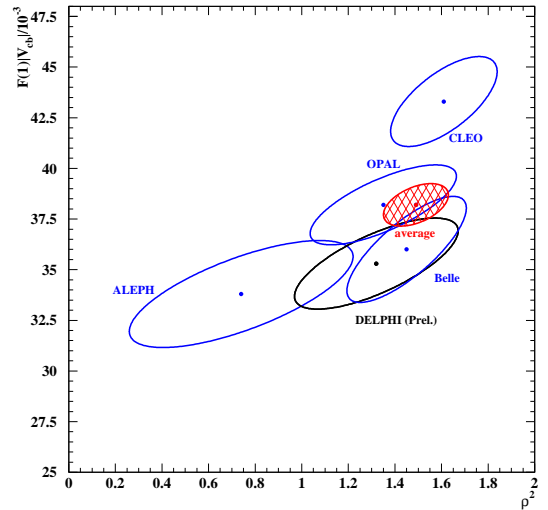


Figure 3: Comparison of $|V_{cb}|$ measurements from various experiments. Plotted is $\mathcal{F}(1)|V_{cb}| \times 10^3$ versus the form-factor slope parameter ρ^2 .

From the data in the bottom plot of Fig. 2 we extract $\mathcal{F}(1)|V_{cb}| = (4.31 \pm 0.13 \pm 0.18) \times 10^{-2}$

and the form-factor slope parameter $\rho^2 = 1.61 \pm 0.09 \pm 0.21$ with a χ^2 fit. The curvature of $\mathcal{F}(w)$ is constrained as predicted from ⁷. Using the charged to neutral ratio for B-mesons at the $\Upsilon(4S)$, $f_{+-} = 0.521 \pm 0.012$, to average over both modes and $\mathcal{F}(1) = 0.919^{+0.030}_{-0.035}$ from HQET we extract ⁸ :

$$|V_{cb}| = (4.69 \pm 0.14 \pm 0.20 \pm 0.18) \times 10^{-2}$$

The errors are statistical, systematic and theoretical. In Fig. 3 we compare our result with similar analysis from the LEP experiments and from BELLE. One should take into account that there are differences between the analysis. The efficiency for the pion detection from the subsequent D^* decay are different for the LEP- and $\Upsilon(4S)$ -experiments, CLEO measures both charged and neutral D^* , LEP only charged ones, and CLEO fits for background from $\bar{B} \rightarrow D^* X l \bar{\nu}$ while LEP uses a model. A 2σ - fluctuation in the latter alone can explain the differences between LEP and CLEO ⁹. This example illustrates very well the importance of over constraining not only each parameter of the mixing matrix but also each measurement in order to get a really good understanding of all systematic aspects which limit the precision of the measurements.

2.2 $|V_{cb}|$ inclusive

An alternative approach to get $|V_{cb}|$ is using measurements of the inclusive semileptonic decay rate $B \rightarrow X_c l \bar{\nu}$. Although there are fewer details of the hadronic final state to be considered in inclusive measurements, non-perturbative effects do still affect the $|V_{cb}|$ extraction from the measured rates. Again, HQET is used to control these effects. Using an operator product expansion one can express moments of measured inclusive observables like lepton energy and masses of hadronic final states in terms of HQET parameters $\bar{\Lambda}$, λ_1 and λ_2 . These moments can be thought of as the mass difference between the b -quark and the B -meson ($\bar{\Lambda}$), the kinetic energy of the b -quark inside the B -meson (λ_1) and the hyperfine interaction of the b -spin with the light degrees of freedom (λ_2). By measuring moments of various inclusive distributions and extracting the HQET parameters one can reduce the uncertainties on them and thereby the uncertainty in the extraction of $|V_{cb}|$ which can also be expressed in terms of HQET parameters. To extract the HQET parameters one can also make use of measurements of different quark-level processes which depend on the HQET parameters in similar ways, making the extraction less prone to systematic effects which are specific to semileptonic events. The CLEO collaboration measures the first and the second moment of the photon energy spectrum of radiative $b \rightarrow s\gamma$ decays and combines it with a measurement of the mass moments of semileptonic $b \rightarrow c$ transitions to extract $|V_{cb}|$. The photon energy spectrum from $b \rightarrow s\gamma$ decays is shown in Fig. 4 ¹⁰.

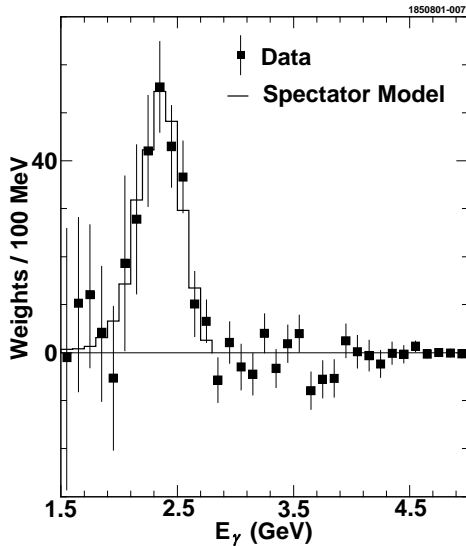


Figure 4: The photon energy spectrum from inclusive $b \rightarrow s\gamma$ decays as measured by CLEO.

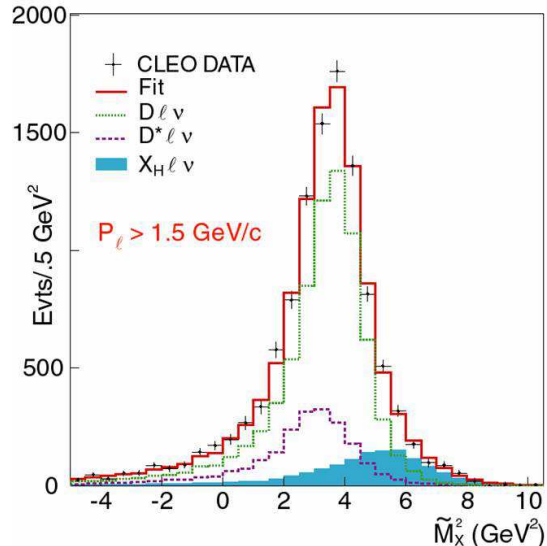


Figure 5: The mass spectrum M_x^2 for $B \rightarrow X_c l \bar{\nu}$ transitions as measured by CLEO.

The moments we extract from this are $\langle E_\gamma \rangle = (2.346 \pm 0.032 \pm 0.011) \text{ GeV}$ and $\langle E_\gamma^2 \rangle - \langle E_\gamma \rangle^2 = (0.0226 \pm 0.0066 \pm 0.0020) \text{ GeV}^2$. In a second analysis we measure the moments of the mass spectrum of the hadronic final state of $\bar{B} \rightarrow X_c l \nu$ decays, shown in Fig. 5, using the hermeticity of the detector to reconstruct the neutrino. We get¹¹ $\langle (M_x^2 - M_D^2) \rangle = (0.251 \pm 0.023 \pm 0.062) \text{ GeV}^2$ and $\langle (M_x^2 - \langle M_x^2 \rangle) \rangle = (0.576 \pm 0.048 \pm 0.163) \text{ GeV}^4$. Combined with theoretical expressions for the first hadronic mass moment¹² these measurements provide a constraint on the HQET parameters $\bar{\Lambda}$ and λ_1 as shown in Fig. 7. The numerical values for the first and the second HQET parameter we get from this are $\bar{\Lambda} = (0.35 \pm 0.07 \pm 0.10) \text{ GeV}$ and $\lambda_1 = (-0.236 \pm 0.071 \pm 0.078) \text{ GeV}^2$. Using these values, combined with a the theoretical expression for the semileptonic decay width Γ_{sl} , and the measured value for the width, $\Gamma_{sl} = (0.427 \pm 0.020) \times 10^{-10} \text{ MeV}$, which we get from the total semileptonic branching ratio $\mathcal{B}(B \rightarrow X_c l \nu) = (10.39 \pm 0.46)^{13}$, and combined with the B -lifetime $\tau_{B^0} = (1.653 \pm 0.028)^{14}$ we extract :

$$|V_{cb}| = (4.04 \pm 0.09 \pm 0.05 \pm 0.08) \times 10^{-2}.$$

Under the assumption of quark-hadron duality this represents a 3.2 % measurement of $|V_{cb}|$. In a third analysis we measure the inclusive lepton energy spectrum in semileptonic B decays. In Fig. 6 we show the measured spectrum which has $B\bar{B}$ -backgrounds subtracted using tuned monte carlo simulations and $e^+e^- \rightarrow qq$ -backgrounds subtracted using events recorded below the $\Upsilon(4S)$ resonance. The spectra have also been corrected for efficiencies, detector resolutions, the motion of the B in the lab frame and final state radiation.

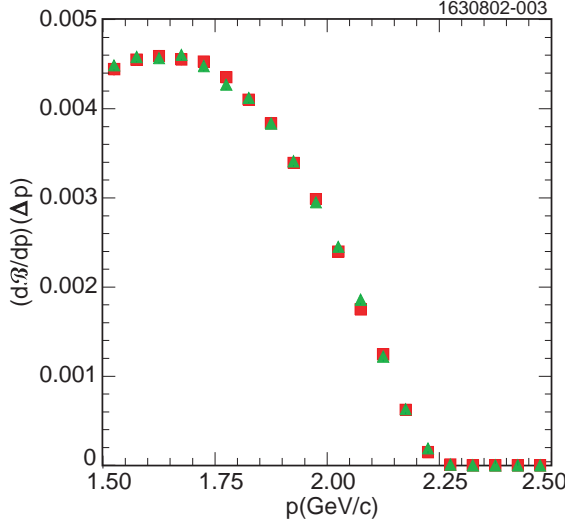
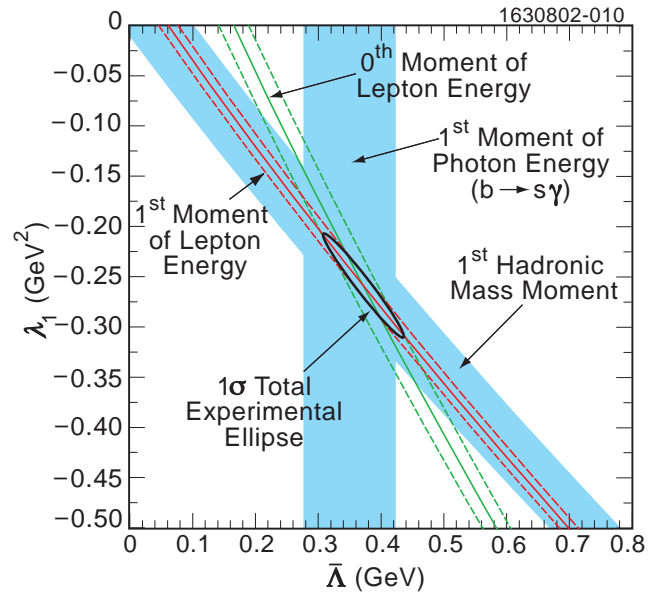


Figure 7: (right) Two-dimensional representation of the λ_1 - $\bar{\Lambda}$ plane with experimental results and their errors on these observables shown as bands and the central value and its error shown as an ellipse. The solid vertical band is from the first moment of the photon energy spectrum in inclusive $b \rightarrow s\gamma$ decays. The solid diagonal band is from the first moment of the mass spectrum in inclusive semileptonic $b \rightarrow c$ transitions. The constraints from the lepton energy spectrum is indicated by lines. All bands overlap in a single region, demonstrating the self-consistency of the HQET parameter extraction.

Figure 6: (left) The corrected energy spectrum at the endpoint for muons (red squares) and electrons (green triangles) in the B -meson rest-frame from semileptonic $b \rightarrow c$ transitions. $d\mathcal{B}$ represents the differential semileptonic branching fraction in the bin Δp , divided by the number of B -mesons in the sample.



We compute the generalized moments :

$$R_0 = \frac{\int_{1.5}^{1.7} \frac{d\Gamma}{dE_{sl}} dE_l}{\int_{1.5}^{1.7} \frac{d\Gamma}{dE_{sl}} dE_l} = 0.6187 \pm 0.0014 \pm 0.016 ; R_1 = \frac{\int_{1.5}^{1.7} E_l \frac{d\Gamma}{dE_{sl}} dE_l}{\int_{1.5}^{1.7} \frac{d\Gamma}{dE_{sl}} dE_l} = 1.7810 \pm 0.0007 \pm 0.0009 \text{ GeV}$$

where the errors are statistical and systematic. Using HQET we extract from these moments $\bar{\Lambda} = (0.39 \pm 0.03 \pm 0.06 \pm 0.12) \text{ GeV}$ and $\lambda_1 = (-0.25 \pm 0.02 \pm 0.05 \pm 0.14) \text{ GeV}^2$.

As shown in Fig.7 the values agree with the ones extracted from the photon energy and the

hadronic mass spectrum. Finally, we can extract :

$$|V_{cb}| = (4.08 \pm 0.05 \pm 0.04 \pm 0.09) \times 10^{-2}.$$

Again, the value is in good agreement with the value determined earlier. The agreement of the results is a nice confirmation of the self-consistency of the techniques used.

3 Measurements of $|V_{ub}|$

Determinations of $|V_{ub}|$ are carried out in the same spirit as for $|V_{cb}|$ via the measurement of decay rates for processes with underlying quark-level transition $b \rightarrow u$. Experimentally this is however more challenging since $b \rightarrow c$ transitions present a hundred-fold larger background to $b \rightarrow u$ transitions. As for $|V_{cb}|$ one also uses semileptonic decays $B \rightarrow X_u l \nu$ to determine $|V_{ub}|$ since non-perturbative effects are much smaller and easier to control than in hadronic decays, although typically not to the same level as in $b \rightarrow c$ transitions. The large energy release and the fact that the final state particles are very light make it harder to control these effects theoretically.

3.1 $|V_{ub}|$ exclusive

The exclusive measurement of $|V_{ub}|$ uses $B \rightarrow \pi l \nu$ and $B \rightarrow \rho l \nu$ events. To unambiguously identify these events the neutrino is reconstructed from the missing energy and the missing momentum assuming that all other final state particles are detected.

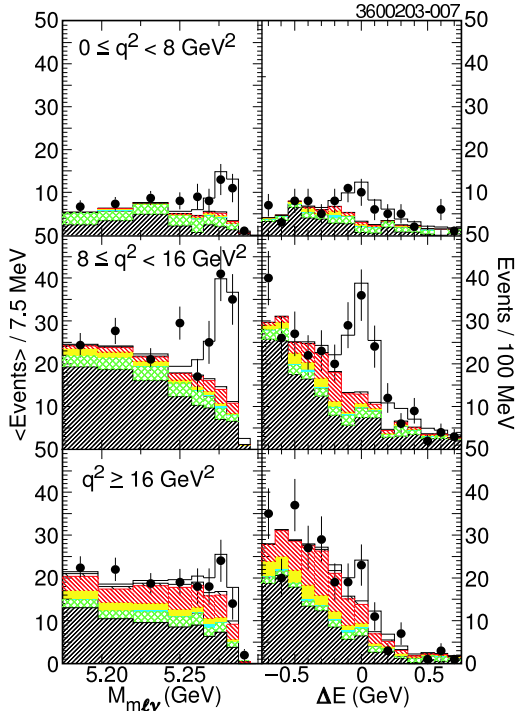


Figure 8: Projections of $M_{ml\nu}$ and ΔE in three different bins of q^2 for the combined π^\pm and π^0 modes.

To better control non-perturbative effects the measurement was performed differentially in the missing energy ΔE , the meson mass $M_{ml\nu}$, the net charge in the event ΔQ , the 2- (3)- π meson mass ranges and q^2 , the momentum transfer of the virtual W in the event. The projections for ΔE and $M_{ml\nu}$ are shown in Fig. 8. The branching ratios we extract from this are :

$$\mathcal{B}(B^0 \rightarrow \pi^- l^+ \nu) = (1.33 \pm 0.18 \pm 0.11 \pm 0.01 \pm 0.07) \times 10^{-4},$$

$$\mathcal{B}(B^0 \rightarrow \rho^- l^+ \nu) = (2.17 \pm 0.34 \pm 0.50 \pm 0.41 \pm 0.01) \times 10^{-4}.$$

where the errors are statistical, experimental systematic, systematic due to residual form-factor uncertainties in the signal, and systematic due to residual form factor uncertainties in cross

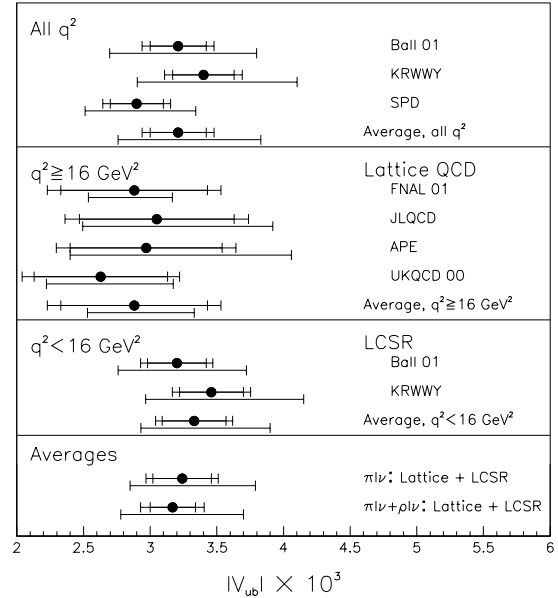


Figure 9: Extracted values for $|V_{ub}|$ from the exclusive semileptonic measurements of the $b \rightarrow ul\nu$ rate in different kinematic ranges using various theoretical approaches.

feed modes respectively. To extract $|V_{ub}|$ from this we employ various theoretical calculations in different q^2 bins to minimize model dependencies. For $q^2 < 16 \text{ GeV}^2$ we use form-factor shapes¹⁶ and normalization results from light-cone sum rules (LCSR) QCD calculations¹⁵ and for $q^2 \geq 16 \text{ GeV}^2$ we use lattice QCD (LQCD)¹⁵ studies. We average over the $\pi l \nu$ and $\rho l \nu$ modes, and also combine, weighted by their errors, the LCSR and the LQCD extractions to get a best estimate of $|V_{ub}|$ ¹⁵:

$$|V_{ub}| = (3.17 \pm 0.17^{+0.16+0.53}_{-0.17-0.39} \pm 0.03) \times 10^{-3}.$$

The errors are statistical, experimental systematic, theoretical systematic from the LCSR and LQCD calculations and $\rho l \nu$ form-factor shape uncertainty, respectively. In Fig. 8 we show the individual results in a graphic representation, demonstrating the very good agreement in different kinematic ranges and using different theoretical calculations.

4 $|V_{ub}|$ inclusive

The inclusive measurement of $|V_{ub}|$ takes advantage of the fact that the u -quark is lighter than the c -quark so that more kinetic energy is released in $b \rightarrow u$ transitions than in $b \rightarrow c$ transitions. Thus the momentum spectrum of final state particles, in particular the lepton momentum spectrum in semileptonic decays, is harder in $b \rightarrow u$ transitions than it is in $b \rightarrow c$ transitions. The relative yield of leptons from $b \rightarrow u$ transitions will therefore be enhanced towards the endpoint of the spectrum. The challenge is to correctly model the shape of the momentum spectrum for both the $b \rightarrow u$ and $b \rightarrow c$ transitions and subtract the latter from the total lepton yield to get the $b \rightarrow u$ contribution. One technique employed by CLEO makes use of the fact that smearing effects which change the shape of the lepton spectrum in $b \rightarrow u$ transitions when going from the parton to the hadron level are very similar to the smearing of the photon energy spectrum in $b \rightarrow s \gamma$ transitions. Thus, we measure this photon energy spectrum and extract a shape function which parameterizes this smearing. This shape function is then used to model the shape of the lepton energy spectrum and separate out the contribution from $b \rightarrow u$ transitions¹⁷.

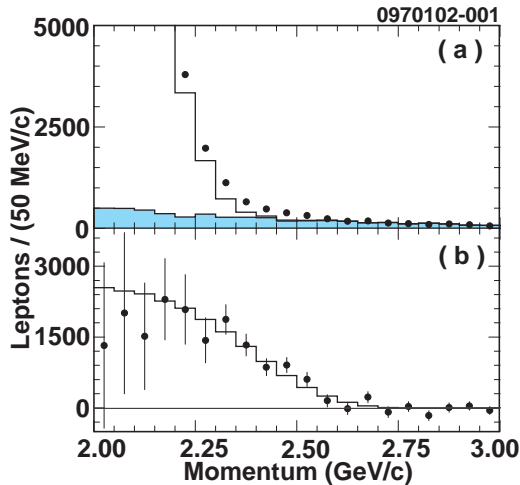


Figure 10: The lepton energy spectrum at the endpoint for semileptonic B decays. The top plot shows the CLEO data (points) compared to $b \rightarrow c$ monte carlo and backgrounds (both histogram). The difference (points in the bottom plot) is due to the $b \rightarrow u$ contribution (solid line in the bottom plot).

The value of $|V_{ub}|$ we extract from the measured rate is¹⁸:

$$|V_{ub}| = (4.08 \pm 0.34 \pm 0.44 \pm 0.16 \pm 0.24) \times 10^{-3}.$$

The first two errors are experimental and the second two errors are from the shape function technique and the $|V_{ub}|$ extraction from the measured $b \rightarrow u$ rate.

The lepton energy is not the only kinematic variable in semileptonic decays which can be used to

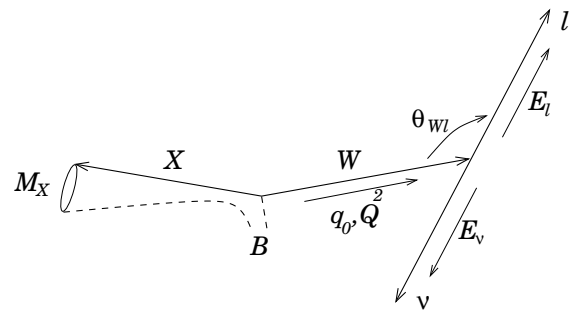


Figure 11: The diagram illustrates the kinematic variables $\cos\theta_{Wl}$, Q^2 and M_x which are used in the three-dimensional fit to measure the $b \rightarrow u$ rate from semileptonic B decays.

separate $b \rightarrow u$ from $b \rightarrow c$ components. The distributions for mass of the hadronic system M_x , the angle between the virtual W and the lepton, $\cos(\Theta_{Wl})$, and the momentum transfer squared to the W , Q^2 , also show distinct differences in shape between $b \rightarrow u$ and $b \rightarrow c$ transitions. To fully exploit this information CLEO uses a fully inclusive three-dimensional fitting technique to measure a rate for $b \rightarrow u$ and extract $|V_{ub}|$. In Fig. 12 we show the mass spectrum of the inclusive semileptonic sample which is used in the fit. In Fig. 13 we show a projection in M_x , just for illustration purpose, for a subsample restricted in all three dimensions of the phase space to the area most sensitive to the $b \rightarrow u$ component. The contribution from $b \rightarrow u$, barely visible in Fig.: 12, becomes much more pronounced. To better control systematic effects we not only fit for the $b \rightarrow u$ component but also include $B \rightarrow D l \nu$, $B \rightarrow D^* l \nu$, $B \rightarrow D^{**} l \nu$ and non-resonant $B \rightarrow X_c l \nu$ components separately. The backgrounds, $b \rightarrow c \rightarrow X l \nu$ decays, $e^+e^- \rightarrow q\bar{q}$ events with a lepton, or fake leptons, from non-semileptonic B decays, are treated as separate background components.

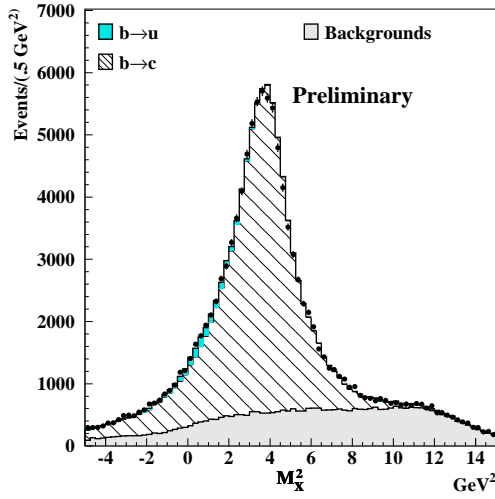


Figure 12: The M_x^2 distribution for the inclusive $|V_{ub}|$ analysis. Note that the $b \rightarrow u$ component is only a tiny part of the entire sample, visible on the left shoulder of the peak in the M_x^2 distribution which is mainly from $b \rightarrow c$ transitions and backgrounds.

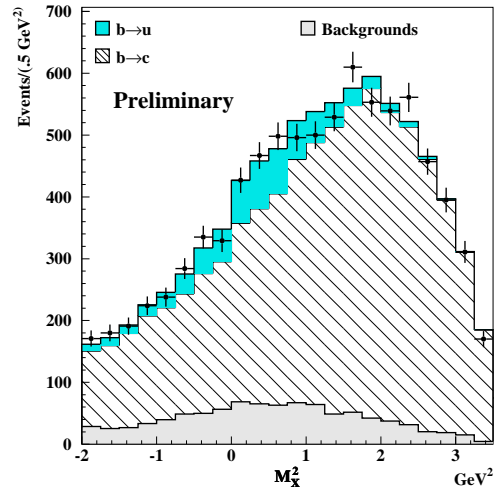


Figure 13: By selecting the region most sensitive to $|V_{ub}|$ in all three dimensions the $b \rightarrow u$ component becomes more pronounced. Note that the shape of the distribution is markedly different for $b \rightarrow u$ and $b \rightarrow c$ transitions.

To get to the total rate for $b \rightarrow u l \nu$ we use HQET to calculate the ratio between the portion of the three-dimensional phase space we cover in this analysis and the total phase space, using the formula $\Delta B_{region} = \mathcal{B}(B \rightarrow X_u l \nu)^{model} \times f_{region}^{HQET}$. From this we extract $|V_{ub}|$ using the relation

$|V_{ub}| = [3.07 \pm 0.12 \times 10^{-3}] \left[\frac{\Delta B_{region}}{0.001 \times f_{region}^{HQET}} \frac{1.6ps}{\tau_B} \right]^{1/2}$ as determined in ¹⁹ which also pioneers the application of the multidimensional cuts used here. Alternative calculations of the conversion factor yield very similar results²⁰. By optimizing the region used to extract $|V_{ub}|$ we can minimize the theoretical uncertainties and get the preliminary result²¹ :

$$V_{ub} = (4.05 \pm 0.18 \pm 0.58 \pm 0.25 \pm 0.21 \pm 0.56) \times 10^{-3} \quad (\text{Preliminary}).$$

The errors are statistical, detector systematics, $B \rightarrow X_c l \nu$ model dependence, $B \rightarrow X_u l \nu$ model dependence and theoretical uncertainties respectively. The result is in agreement with the lepton endpoint analysis from CLEO presented above. There is a slight correlation with that analysis and the errors may be correlated as well. Studies of these correlations, further studies on the optimal region and extraction of moments are in progress.

5 Summary

CLEO uses a broad range of experimental techniques to measure $|V_{ub}|$ and $|V_{cb}|$ in inclusive and exclusive semileptonic B -decays. These measurements, which impose important constraints on the Unitarity Triangle, are always systematically limited. By using different techniques we gain deeper insight into experimental and theoretical details of how to best determine these important quantities. To extract the fundamental parameters $|V_{ub}|$ and $|V_{cb}|$ from measured rates we depend on HQET and lattice QCD. The future CLEO-c program will help to solidify the experimental basis of these theoretical approaches which are essential to progress in the field of heavy flavor physics in general.

Acknowledgments

We gratefully acknowledge the contributions of the CESR staff for providing the luminosity and and the National Science Foundation and the U.S. Department of Energy for supporting this research. The author wishes to thank the organizers of the 'Rencontres de Moriond' for a very exciting and inspiring event.

References

1. N. Cabibbo, Phys. Rev. Lett. **10**, 531 (1963); M. Kobayashi, T. Maskawa, Prog. Theor. Phys. **49**, 652 (1973).
2. L. Wolfenstein, Phys. Rev. Lett. **51**, 1945 (1983).
3. The CLEO Collaboration, Nucl. Inst. Methods Phys. Res. **A320**, 66 (1992); T. S. Hill, Nucl. Inst. Methods Phys. Res., **A418**, 32 (1998).
4. A. V. Manohar and M. B. Wise, *Heavy Quark Physics*, (Cambridge University Press, Cambridge (2000)).
5. K. G. Wilson, Phys. Rev. D **10**, 2445 (1974).
6. S. Hashimoto *et. al.*, Phys. Rev. D **66**, 014503 (2002).
7. I. Caprini, L. Lellouch, M. Neubert, Nucl. Phys. **B530**, 153 (1998).
8. The CLEO Collaboration, Phys. Rev. D **67**, 032001, (2003).
9. ' $|V_{cb}|$ mini-review', in K. Hagiwara *et. al.*, Phys. Rev. D **66**, 010001 (2002), pp 701-706.
10. The CLEO Collaboration, Phys. Rev. Lett. **87**, 251807, (2001).
11. The CLEO Collaboration, Phys. Rev. Lett. **87**, 251808, (2001).
12. A. Falk, M. Luke, M. Savage, Phys. Rev. D **53**, 2491 (1996); A. Falk, M. Luke, Phys. Rev. D **57**, 424 (1998).
13. The CLEO Collaboration, Phys. Rev. Lett. **76**, 1570, (1996).
14. PDG, D. E. Groom *et. al.*, Eur. Phys. J. C **15**, 1 (2000).
15. The CLEO Collaboration, sub. to Phys. Rev. D, hep-ex/0304019 and references therein.
16. P. Ball and R. Zwicky, JHEP **0110**, 019 (2001); P. Ball and V. M. Braun, Phys. Rev. D **58**, 094016 (1998); D. Scora and N. Isgur, Phys. Rev. D **52**, 2783 (1995).
17. M. Neubert, Phys. Rev. D **49**, 3392 (1994); *ibid.*, 4623 (1994); I. I. Bigi *et. al.*, Int. J. Mod. Phys. A **9**, 2467 (1994); A. K. Leibovich, I. Low, I. Z. Rothstein, Phys. Rev. D **61**, 053006 (2000); F. De Fazio, M. Neubert, JHEP **06**, 017 (1999).
18. The CLEO Collaboration, Phys. Rev. Lett. **88**, 231803 (2002).
19. C. W. Bauer, Z. Ligeti, M. E. Luke, Phys. Rev. D **46**, 113004, (2001).
20. M. Neubert, JHEP **0007**, 022 (2000); M. Neubert, T. Becher, Phys. Lett. B **535**, 127 (2002).
21. The CLEO Collaboration, 'Preliminary Results on $|V_{ub}|$ from Inclusive Semileptonic B Decays with Neutrino Reconstruction', Presented at ICHEP02.